# ANALYSIS OF THE OPTICAL LIMITATIONS OF A BEAM MONITOR FOR THE RHIC INJECTION LINE

B. S. Lee

August 1993

Collider Accelerator Department

**Brookhaven National Laboratory**

**U.S. Department of Energy**

USDOE Office of Science (SC)

# DISCLAIMER

# ANALYSIS  OF  THE  OPTICAL  LIMITATIONS  OF  A  BEAM

# MONITOR  FOR  THE  RHIC  INJECTION  LINE

Be-Su Lee*

August 26, 1993

*Chalmers University of Technology, Sweden

# Analysis of the Optical Limitations of a Beam Monitor
# for the RHIC Injection-Line

AGS Department, Brookhaven National Laboratory

26 August 1993

## Abstract

A flourescing target in the beam vacuum pipe provides two-dimensional information on the beam position and profile which is relayed to a video camera behind shielding blocks. Here we study the degradation of the optical imaging and estimate the quality of the picture obtained. Each of the factors limiting the monitor resolution is first treated separately, then folded together to give an expression for the final image resolution of the target. Calculations made are primarily based on Gaussian optics and measurements on the lens system.

## 1. Introduction

Before entering the Relativistic Heavy Ion Collider (RHIC) the ion beam has to be accurately diagnosed and well defined. For this purpose a number of detectors providing information on the position, profile and intensity of the beam are to be installed in the injection-line between the BNL Alternating Gradient Synchrotron (AGS) and the RHIC ring.

A detector system using a fluorescent screen has been designed as a less expensive alternative to harp wire monitors. The image formed when the beam hits the screen is transported by two mirrors to a focusing optical system and a television camera. A framegrabber is then used to store the digitized information for later analysis.

A set-up of this monitor design has been overviewed and carefully aligned in the laboratory. It is now installed in the injection-line between the Booster and the AGS where it will be tested and evaluated.

## 2. Monitor Design

### 2.1 Monitor Set-Up

The fluorescent screen is made of a uniform layer of phosphor, $Gd_2O_2S$:Tb, deposited on a substrate of aluminum foil. Four lines of drill holes forming a rectangular array 60.5 × 85 mm serve as fiducial marks.

*Fig.*1 shows the mechanical construction and set-up of the beam monitor. The screen is inclined 45° to the beam axis, its fluorescing surface facing the beam with a tilt upwards. When monitoring the beam, the screen is inserted into the beam pipe by a pneumatic mechanism. The beam impinges on the screen, excites the phosphor and hence produces an optical image containing full two dimensional information on the beam

intensity and profile. The picture is transported by two plane front surface mirrors to the television camera mounted behind shielding blocks at the wall.

The picture of the phosphor screen is imaged and focused onto a CCD camera (SONY XC-57 H/V) by a 385 mm telephoto lens (Century Tele-Athenar II, TN 3845). An aperture in the telephoto lens with the range 4.5 − 32 can be adjusted manually thus allowing some control of the light impinging on the CCD screen. The field of view and magnification of the optical system is fixed by the positions of the television lens and the camera.

## 2.2 Field of View and Magnification

The magnification $M$ is determined by the focal length and the distance from the second principal plane of the optical system to the image screen. In our monitor set-up, the telephoto lens and the television camera are positioned so that the array of fiducial marks on the phosphor screen covers the *width* of the television screen. The projected image of the array of reference marks is a square while the CCD screen and the television picture are standardized at a 4-to-3 width-to-height ratio. This means that we will get a loss in height when viewing the screen. Only one of the horizontal lines with fiducial marks can be seen in the same picture.

The sensing area of the CCD (same as the 2/3 inch camera tube) is 8.8 × 6.6 mm. The horizontal and vertical dimensions of the array of fiducial marks are 60.5 mm and 85 mm ($\approx 60\sqrt{2}$ mm) respectively. In our monitor set-up, the picture viewed at is estimated to be about 61 mm wide and 46 mm high which corresponds to an optical magnification $M$ of $8.8/61 \approx 0.14$.

# 3. Model of the Optical System

## 3.1 Modelling the Telephoto Lens

Not knowing what elements are included in the television lens, one must treat the optical system as a black box. Surface-by-surface calculations which are needed for calculating third order effects like lens aberrations cannot be performed. However, the position and size of the image formed by the optical system can be readily determined when the cardinal points are known. Refer to section 3.2, "Image Position and Height", for more detailed information.

Experiments in order to characterize the television lens have been made in the laboratory. A model based on first order optics and principal planes was used. *Fig.*2 summarizing the experimental results shows the determined positions of the cardinal points. The physical end of the telescope is used as a landmark for references.

The quantity (385 mm) listed as focal length in the specifications is the effective focal length (EFL) which is defined as the distance between the back focal point and the back principal point. If we assume that all components in the lens only have spherical surfaces, it can be shown that the EFL on the object side and the EFL on the image side are equal even though the lens is not symmetric. (In *Fig.*2 the two distances are labeled $f$). We can then reduce the number of independent unknown quantities to two: distances $\overline{F_o P}$ and $\overline{F_i P}$. In other words, measurements relating the positions of the front and back focal points to a landmark on the lens are sufficient to fully characterize the system with Gaussian optics.

A 1/4-inch fibre optical cable terminated with a pin-hole aperture a few tenths of a millimeter in diameter served as a light source in our experiments. To produce a bundle of parallel rays it was placed at the focal

point of an achromatic lens with a focal length of 6 inches. Tests ensured that the beam was satisfactorily collimated and did not widen.

Careful alignments were then made with the horizontally mounted telephoto lens and a small plate was placed downstream of the set-up perpendicular to the optical axis. The position of the focal point was determined by sliding the plate along the optical axis. When a sharp spot was imaged on the plate the distance from the plate to the physical end of the television lens was measured with a non-elastic string. This procedure was repeated several times (typically six) to attain a statistical value. Measurements were made for both sides of the telescope and also for some different adjustments of the lens. The positions of the focal points were found to vary slightly when changing the power. The values listed in *Fig.2* apply for a lens focusing at 20 ft which is the same power as in the real set-up.

The uncertainty in the statistical values for $\overline{F_i P}$ and $\overline{F_o P}$ is estimated to about 1/10 inch. Thus, we get

$$
\begin{aligned}
\overline{F_i P} &= (16.1 \pm 0.1)'' && \text{from direct measurements} \\
\overline{F_o P} &= (15.3 \pm 0.1)'' && \text{from direct measurements} \\
\overline{H_i P} &= (0.94 \pm 0.1)'' && \text{calculated} \\
\overline{H_o P} &= (0.14 \pm 0.1)'' && \text{calculated} \\
\overline{H_i H_o} &= (1.1 \pm 0.2)'' && \text{calculated}
\end{aligned}
$$

where $P$ = reference point (intersection between physical end of telescope and optical axis), $H_o$ = first principal point, $H_i$ = second principal point, $F_o$ = first focus point, $F_i$ = second focus point, $f$ = effective focal length (EFL).

## 3.2 Image Position and Height. Checking Our Model.

The location and size of an image, produced by an optical system without aberrations, can be readily determined when the cardinal points are known. *Fig.3* shows how a simple ray construction can be used to locate a Gaussian image point.

The lateral or transverse magnification $M$ is defined as the ratio of image size to object size, i.e.

$$
M \equiv \frac{h'}{h}
$$

From similar triangles in *Fig.4* we get:

$$
\frac{h'}{h} = \frac{f}{x} \tag{1}
$$

$$
\frac{h'}{h} = \frac{x'}{f'} \tag{2}
$$

$$
\frac{h'}{h} = \frac{s'}{s} \tag{3}
$$

For an optical system in air, consisting of elements with spherical surfaces only, $f$ is equal to $f'$. The locations of the focal points relative the object and image are then (use equation (1) and (2)) given by the formula

$$
f^2 = xx' \tag{4}
$$

The rays (1), (2) and (3) in the figure correspond to equations (1), (2) and (3) respectively. In the paraxial region these expressions are equivalent and should yield the same values. The errors in the quotients

3

on the right-hand side of the equations are, however, different. As distances $x'$ and $s'$ are much smaller then distances $x$ and $s$, their relative errors are larger. For these reasons, though equations (1), (2) and (3) are theoretically equivalent, equation (1) is preferred when determining the magnification $M$.

Numerical values and information on the monitor set-up are given in *Fig.*1 and *Fig.*2. Assuming an accuracy of $1/8''$ in the shorter distances and $1/4''$ in the longer distances we get

$$x = (16\frac{1}{16}'' + 92\frac{3}{4}'' + 29\frac{1}{4}'') - 15.3'' = (122.763 \pm 0.9)''$$

$$s = x + f = 122.763'' + 385mm = (137.920 \pm 0.9)''$$

$$x' = (17\frac{3}{16}'' + \frac{9}{16}'') - 16.1'' = (1.65 \pm 0.4)''$$

$$s' = x' + f = 1.65'' + 385mm = (16.807 \pm 0.4)''$$

which inserted in expressions (1), (2) and (3) give

$$\frac{f}{x} = (0.123 \pm 0.002)''$$

$$\frac{x'}{f} = (0.11 \pm 0.03)''$$

$$\frac{s'}{s} = (0.12 \pm 0.01)''$$

The fact that the three quotients agree within error bars is a strong indication of the measurements being satisfactorily performed. However, the obtained value for the magnification, $M = 0.12$, is 14% off from the actual magnification, $M = 0.14$. This discrepancy may be due to the focal length changing with the power of the lens. When locating the principal points two distances were subtracted on each side of the lens. According to *Fig.*2, $\overline{F_x P}$ (where $x$ stands for $o$ when on the object side and $i$ when on the image side) minus $\overline{F_x H}$ is equal to $\overline{H_x P}$. The distance $\overline{F_x P}$ was directly measured for the lens having the same power as in our monitor set-up, while the effective focal length $\overline{F_x H}$ was taken as equivalent to the focal length in the specifications. This assumption may involve some error. As the positions of the principal planes usually vary when the focus lens group is moved, the focal length in the monitor set-up (focusing at 20 ft) may not be the same as the specified value (focusing at infinity).

## 4. Limits to the Resolution

### 4.1 Quality of Optics in Telephoto Lens

Lens aberrations cannot be computed and mathematically evaluated since we do not know what type of components are included in the lens. However, the manufacturer provides some technical data on the lens system: according to the specifications, the line resolution is about 100 l/mm. This figure has been obtained by viewing a target consisting of different patterns of evenly spaced black and white bars. A blur in the image can just be detected when the diameter of circle of confusion is equal to the distance between two resolvable lines. In other words, a line resolution of 100 l/mm corresponds to a permissible diameter of circle of confusion twice the reciprocal of the line frequency, i.e. 20 $\mu$m. We may expect the blur occurring in our final image to be larger than this value, since the picture of the phosphor screen has less contrast than the target used in the resolution tests. The monitor resolution of the screen is thus expected to be degraded by more than $20/M = 143$ $\mu$m.

Note: The viewing distance of the target in the resolution tests plays a less important role for telescopic

systems since the angles subtended by the rays in object space are very small. For most applications the resolution specified can be used.

## 4.2 Video Camera Limitations

The display of two fields at a rate of 60 fields per second produces a complete, interlaced image at a rate of 30 frames per second. Each picture or frame consists of 525 lines which yields 510 picture elements in the horizontal direction and 492 pixels vertically. According to the camera specifications this will provide a H/V resolution of 380 and 485 lines respectively. The area of the camera tube is specified as 8.8 × 6.6 mm. This means that the permissible diameter of circle of confusion on the CCD screen is $2 \cdot (8.8/380) = 46$ $\mu$m in the horizontal direction and $2 \cdot (6.6/485) = 27$ $\mu$m in the vertical direction. By compensating for the optical magnification $M$, we obtain a contribution to the overall monitor resolution 46/M= 330 $\mu$m horizontally and 27/M= 194 $\mu$m vertically.

## 4.3 Depth of Field Limitations

Since the screen is tilted 45°, light emitted from points at different heights on the phosphor screen travel different distances along the optical axis. The optical system can only provide a limited depth of field, which means that, if the center of the screen is imaged sharply, the resolution decreases with the height of the detected beam. A point not in focus will appear as a disc in our final image. Using Gaussian optics the diameter of the blur, $\phi$, is calculated as

$$\phi = A \cdot \frac{\Delta/s}{(s/f - 1)(1 + \Delta/s)} \tag{5}$$

$A$ = effective aperture of the optical system
$s$ = distance between the center of the phosphor screen and the first principal plane
$f$ = effective focal length
$\Delta$ = offset along the optical axis from the center of the screen

*Fig.*4 shows, for some different F-numbers, how big a blur the limited depth of field will produce on the CCD screen ($f = 385$ mm, $s = 138$ in., $\Delta = h$). The diameter of circle of confusion $\phi$ is given as a function of the height $h$ measured from the optical axis. From the figure, we may conclude, that the size of the blur spot is as good as directly proportional to the beam size.

In the calculations, we have assumed the diameter $A$ of the effective aperture stop to be the same as the clear aperture of the lens. The latter can easily be calculated, since we know that the F-number or the relative aperture is defined as the ratio of the effective focal length to the clear aperture.

The maximum blur size, $\phi$, in the image can also be expressed as a function of the depth of field, $d$, and the relative aperture, F. When $d \ll s$:

$$\phi = A \cdot \frac{d/(2s)}{s/f - 1} \approx 6.78 \cdot 10^{-3} \left( \frac{d}{F} \right) \tag{6}$$

This alternative formulation is useful when we are interested in how large the permissible diameter of the circle of confusion is for a certain depth of field, for instance, the depth of field needed to image the whole field of view acceptably sharp. In our beam monitor the field of view is 46 mm in the vertical direction. Since the target is tilted 45°, the picture produced by the flourescing screen extends the same distance along the optical axis as it extends vertically. As a numerical example, assume that the lens is working at F/5.6.

The depth of field covers the whole field of view, i.e. is equal to 46 mm, if the permissible diameter of circle of confusion is 56 $\mu$m. This would correspond to the depth of field limitations contributing to the monitor resolution with $56/M = 398$ $\mu$m.

## 4.4 Mechanical Vibrations

The second mirror, the television lens and the camera are all attached to a plate mounted on the wall. Vibration levels of significance are hardly liable to occur in these components. The first mirror, on the other hand, is much more easily disturbed. The rails connected to its mirror mount are directly bolted to stands on the beam pipe. Water running nearby in the cooling system causes the installed monitor to vibrate. We now investigate how these motions affect the optical image from the phosphor screen.

The solid lines in *Fig.*5 shows the undisturbed light path. We start with examining the effects of pure translative motions of the first mirror. It can easily be realized that in-plane translations do not change the image. The rays will only hit identical points on the plane mirror surface. Movements of the mirror normal to its plane, on the other hand, result in the light path being directly translated. The offset in the final image is, however, of the same order of magnitude as the disturbances in the mirror. For instance, a displacement $d$ of the first mirror in its normal direction produces an offset $d\sqrt{2}$ of the image at the telephoto lens.

We now examine the effects of changing the tilt of the first mirror. The rails attached to the mirror mount can be assumed to pivot around points lying a distance $L_{\mathrm{piv}}$ from the center of the mirror. A small displacement $u$ of the rails at the height of the mirror center corresponds to changing the tilt of the mirror an angle $\delta_1 = u/L_{\mathrm{piv}}$. The light incident on the errored mirror are deflected an additional angle $\delta_2 = 2\delta_1$ relative to its original path. The dashed lines in *Fig.*5 show how the distances $L_2$ and $L_3$ act as level arms, increasing the offset from the optical axis as the light travels. Since $\delta_2 = \delta_3$, this increase is directly proportional to the distance traveled from the first mirror. If the translation of the mirror also is considered, the total offset of the image at the telephoto lens is given by

$$
\begin{aligned}
\Delta &= L_2\delta_2 + L_3\delta_3 + u \\
&= 2\delta_1(L_2 + L_3) + u \\
&= \left(\frac{2(L_2 + L_3)}{L_{\mathrm{piv}}} + 1\right) u
\end{aligned}
\tag{7}
$$

Because it takes a certain time for the flourescing phosphor to decay, light emitted from points on the phosphor screen images as blurred spots with coma-like tails. The faster the absolute position of the picture varies, the more blurred will the image appear.

The degradation of the image resolution can readily be determined if the vibrations are assumed to be harmonic. A displacement $u = A\sin\omega t$ of the first mirror produces, according to equation (7), a change in absolute position of the picture,

$$
\Delta = \left(\frac{2(L_2 + L_3)}{L_{\mathrm{piv}}} + 1\right) A\sin\omega t
\tag{8}
$$

at the lens. By differentiating the expression, the maximum length $l$ of the coma-like blur is obtained as

$$
l = 2\pi A \left(\frac{2(L_2 + L_3)}{L_{\mathrm{piv}}} + 1\right) \frac{\tau}{T} \leq 2A \left(\frac{2(L_2 + L_3)}{L_{\mathrm{piv}}} + 1\right)
\tag{9}
$$

where $\tau$ is the phosphor decay time and $T = 2\pi/\omega$ is the time period of the vibrations.

Note that the image resolution width of the phosphor screen is approximately the same as the length of the blurred spot at the lens. The quantity $l$ given by expression (9) thus represents the contribution to the system resolution due to mechanical vibrations.

Finally, we insert numerical values: $L_{\text{piv}} = 34''$ and distances listed in *Fig.*1. According to equations (7) and (9), we get an offset

$$\Delta = \left(\frac{2(92.75 + 29.25)}{34} + 1\right) u = (7.2 + 1)u = 8.2u$$

and a maximum blur size

$$l = 51.4 \cdot A \cdot \frac{\tau}{T} \tag{10}$$

The decay time $\tau$ of the phosphor is about 1 ms. As an example, assume a vibration amplitude $A = 0.1$ mm and a vibration period $T = 100$ ms. A maximum blur length or size of 51 $\mu$m is then obtained.

## 5. Final Resolution

The energy distribution in the blurred image of an object point can be approximated as Gaussian. Each contribution to the monitor resolution is then added in quadrature. The final resolution, $\sigma_{sys}$, is thus obtained as

$$\sigma_{sys} = \sqrt{\sigma_{opt}^2 + \sigma_{cam}^2 + \sigma_{dof}^2 + \sigma_{vib}^2} \tag{11}$$

To get an expression for the highest resolution which can be obtained all over the object, insert:

$$
\begin{aligned}
\sigma_{opt} &= 143\mu\text{m} \\
\sigma_{cam} &= 330\mu\text{m} \\
\sigma_{dof} &= \left(\frac{48.4}{F}\right)\sigma \\
\sigma_{vib} &= 51.4 \cdot A \cdot \frac{\tau}{T}
\end{aligned}
$$

where $\sigma$ is the beam size in mm, $A$ is the amplitude of the mechanical vibrations of the mirror, $\tau$ is the phosphor decay time and $T$ is the time period of the vibrations.

## 6. Summary

A beam monitor with a fluorescent screen as a target has been designed for use in the RHIC injection-line. Two mirrors guiding the picture over a distance of about 4 m allow the video camera to be placed behind shielding blocks. The field of view provided by the monitor is 61 × 46 mm and the optical magnification is 0.14.

A model, based on measurements in the laboratory and Gaussian optics, has been developed for the optical system. The model provides data required for evaluating the system performance. In a study on degradations of the image, we discuss the quality of the optics, video camera limitations, depth of field (dof) limitations and mechanical vibrations. Each of these factors produces, when imaging a point, a certain image

7

broadening which width has been estimated. Finally, we have made an attempt to fold these contributions together to obtain an overall image resolution, $\sigma_{sys}$. The obtained expression for $\sigma_{sys}$ can be interpreted as a base resolution of about 360 $\mu$m due to the detector optics and size of the CCD pixels, and a contribution in quadrature of $\sigma_{dof}$, a quantity proportional to both the beam size and the relative aperture of the lens. In most applications, the size of the pixels and the limited field of depth contribute the most of $\sigma_{sys}$, while lens aberrations and mechanical vibrations play a less important role.

## 7. Figure Captions

**Fig.1:** Beam monitor design.

**Fig.2:** Location of Gaussian points of telephoto lens. The positions of the focal points have been measured, while the focal length $f$ is provided by lens specifications.

**Fig.3:** Ray construction to locate Gaussian image point.

**Fig.4:** Size of blur spot imaged on CCD screen due to limitations of depth of field. The diameter of circle of confusion is given as a function of the height of the object point relative the optical axis. The relative aperture is included as a parameter.
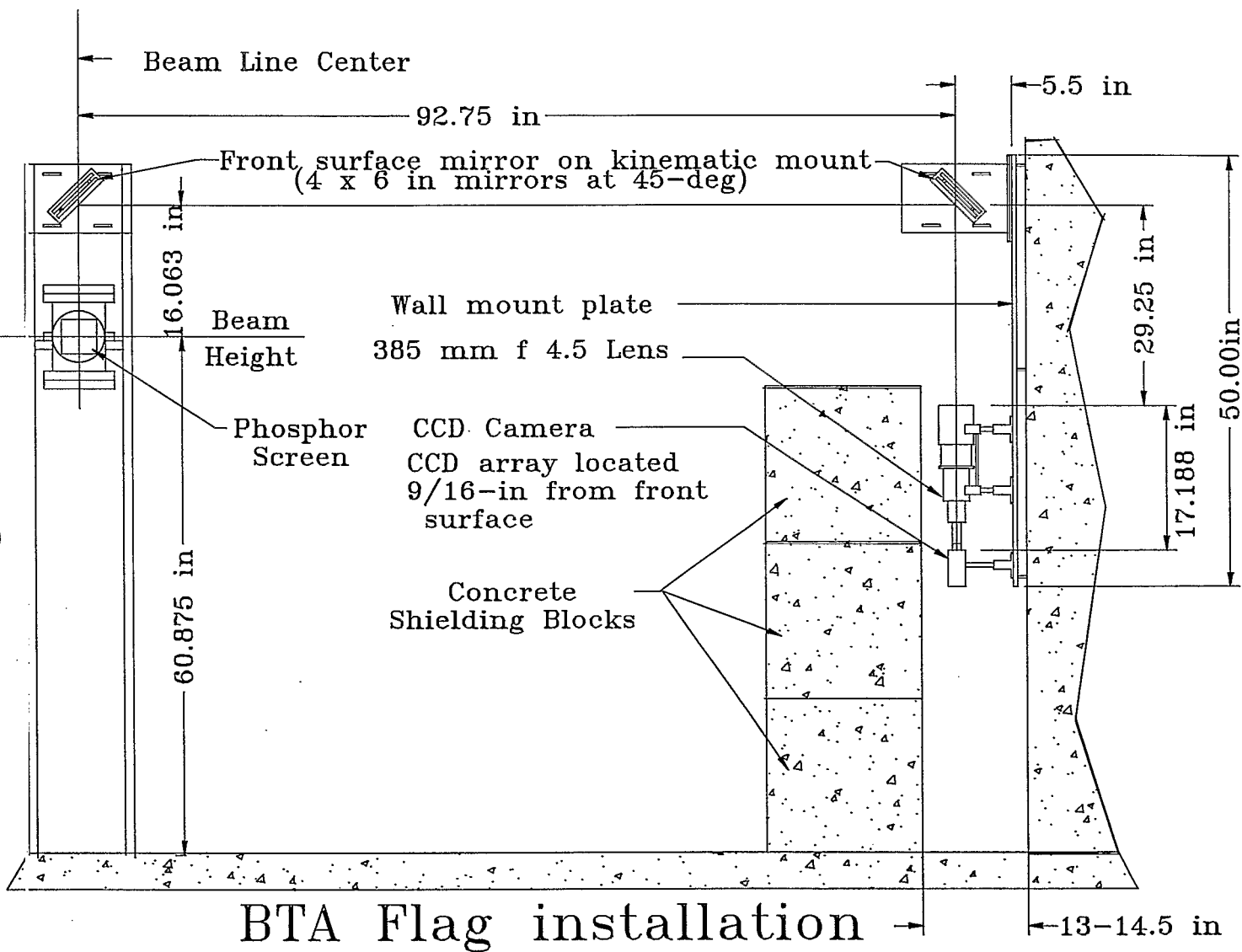
**Fig.5:** Change in ray path due to a change in inclination of the first mirror. The solid lines represent the original light path and the dashed lines the errored path.

## Acknowledgements

## References

[1] W.J. Smith, *Modern Optical Engineering.* McGraw-Hill, 1966.

[2] A. Horder, *The ILFORD Manual of Photography*, 5th Edition. Ilford Limited, 1958.

[3] E. Hecht, A. Zajac, *Optics.* Addison-Wesley Publ. Comp., 1974.

[4] D.L. Cannon, *Understanding Communications Systems.* Texas Instruments Publ. Cent., Dallas 1984.

[5] Franz-Josef Decker, *Beam Size Measurements at High Radiation Levels*, Proc. 1981 Particle Accelerator Conf., 91CH3038-7, P 1192, (1991)

[6] D.P Russell, K.T. McDonald, *A Beam-Profile Monitor for the BNL Accelerator Test Facility (ATF)*, Proc.1989 IEEE Particle Accelerator Conf., 89CH2669-0, P 1510, (1989).

[7] M.C. Ross, *High Resolution Beam Profile Monitors in the SLC*, Proc. IEEE Transactions on Nuclear Science, Vol. NS-32, No.5, P 2003, (1985).

[8] Melles Griot, *Optics Guide 5*, 1990.

Beam Line Center

92.75 in
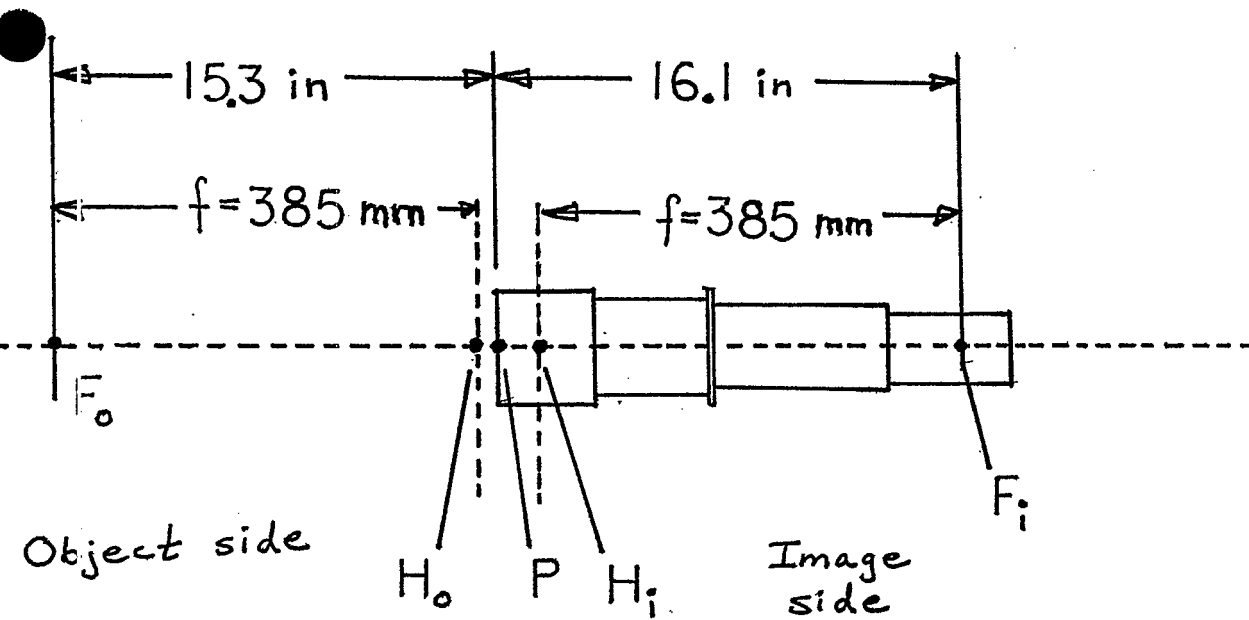
5.5 in
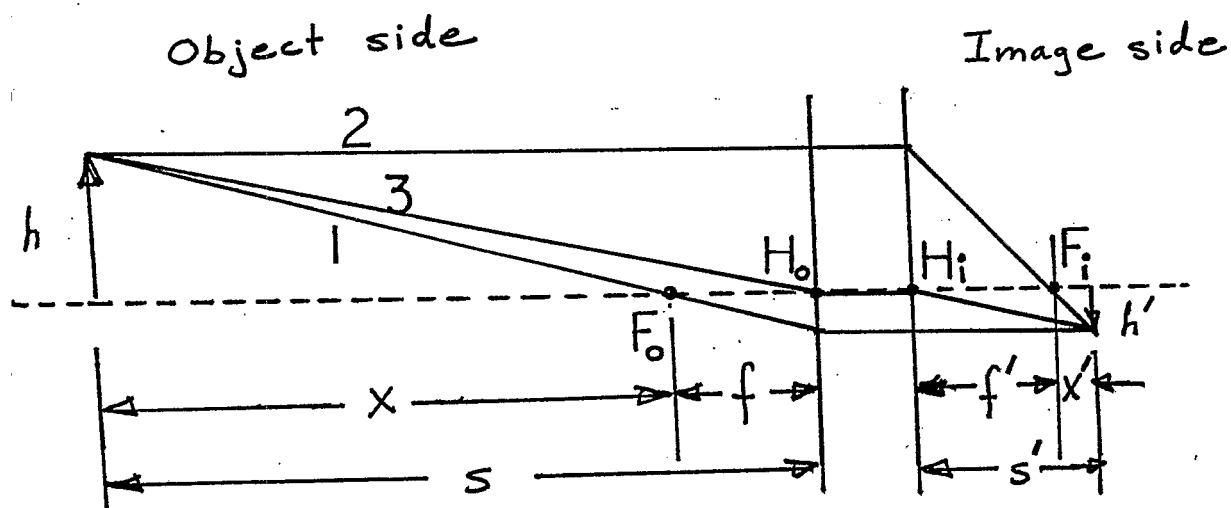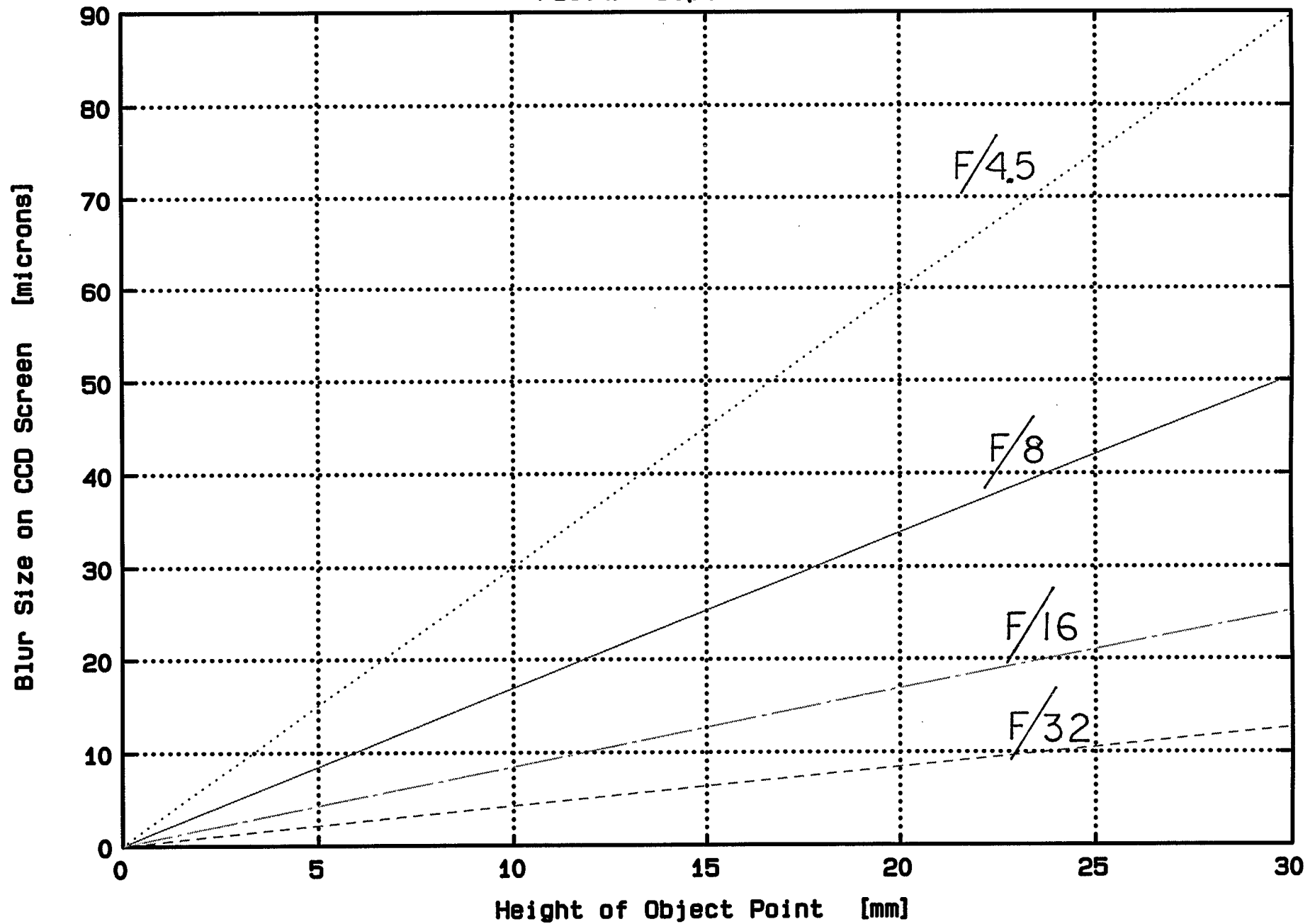
Front surface mirror on kinematic mount
(4 x 6 in mirrors at 45-deg)

16.063 in

Beam
Height

Wall mount plate

385 mm f 4.5 Lens

29.25 in

50.00in

Phosphor
Screen

CCD Camera

CCD array located
9/16-in from front
surface

17.188 in

Concrete
Shielding Blocks

60.875 in

BTA Flag installation

13-14.5 in

Figure 1

FIG. 2



FIG. 3

FIG.4:   Depth of Field

$$\delta_2 = 2 \delta_1$$
$$\delta_3 = \delta_2$$

Figure 5